

# A method for treating the passage of a charged hard sphere ion as it passes through a sharp dielectric boundary

Dezső Boda,<sup>1,2,a)</sup> Douglas Henderson,<sup>2</sup> Bob Eisenberg,<sup>3</sup> and Dirk Gillespie<sup>3</sup>

<sup>1</sup>*Department of Physical Chemistry, University of Pannonia, P.O. Box 158, H-8201 Veszprém, Hungary*

<sup>2</sup>*Department of Chemistry and Biochemistry, Brigham Young University, Provo, Utah 84602, USA*

<sup>3</sup>*Department of Molecular Biophysics and Physiology, Rush University Medical Center, Chicago, Illinois 60612, USA*

(Received 31 March 2011; accepted 17 July 2011; published online 12 August 2011)

In the implicit solvent models of electrolytes (such as the primitive model (PM)), the ions are modeled as point charges in the centers of spheres (hard spheres in the case of the PM). The surfaces of the spheres are not polarizable which makes these models appropriate to use in computer simulations of electrolyte systems where these ions do not leave their host dielectrics. The same assumption makes them inappropriate in simulations where these ions cross dielectric boundaries because the interaction energy of the point charge with the polarization charge induced on the dielectric boundary diverges. In this paper, we propose a procedure to treat the passage of such ions through dielectric interfaces with an interpolation method. Inspired by the “bubble ion” model (in which the ion’s surface is polarizable), we define a space-dependent effective dielectric coefficient,  $\epsilon_{\text{eff}}(\mathbf{r})$ , for the ion that overlaps with the dielectric boundary. Then, we replace the “bubble ion” with a point charge that has an effective charge  $q/\epsilon_{\text{eff}}(\mathbf{r})$  and remove the portion of the dielectric boundary where the ion overlaps with it. We implement the interpolation procedure using the induced charge computation method [D. Boda, D. Gillespie, W. Nonner, D. Henderson, and B. Eisenberg, *Phys. Rev. E* **69**, 046702 (2004)]. We analyze the various energy terms using a spherical ion passing through an infinite flat dielectric boundary as an example. © 2011 American Institute of Physics. [doi:10.1063/1.3622857]

## I. INTRODUCTION

It is well known that the electrostatic energy diverges when a point charge approaches a sharp dielectric boundary. Such a boundary separates two domains with piecewise constant dielectric coefficients. In the implicit solvent approach, electrolytes are commonly modeled by the primitive model (PM) where ions are charged hard spheres and the solvent is a continuum dielectric. Each charged hard sphere has a point charge at its center. The surface of this sphere is electrostatically inactive: the sole purpose of this surface is to prevent ions from overlapping. From an electrostatic point of view, a charged hard sphere is a point charge. Therefore, when an ion overlaps with the dielectric boundary, the point charge in its center approaches the boundary, the energy diverges, and this representation becomes unrealistic.

For this reason, simulations of the PM electrolyte near a dielectric interface have been, to the best of our knowledge, mostly performed with ions that cannot overlap with the boundaries.<sup>1–17</sup> The dielectric boundaries usually were hard impenetrable walls or ions were excluded from their vicinity by other walls or some repulsion potential. Even when the possibility of ions crossing dielectric boundaries is otherwise a physical reality, authors decided to avoid such events in their simulations in one way or other. A few representative examples are the following.

In our ion channel simulations,<sup>11,12,14,17</sup> we used a dielectric coefficient inside the channel that was equal to that of the bath. A similar approach was followed by Coalson and co-workers.<sup>18,19</sup> In reality, the dielectric coefficient is smaller in the channel pore than in the bath. This manifests itself in two major effects. (1) Pair interactions between ions inside the pore are stronger than between ions outside the pore because they are less screened by the smaller dielectric coefficient. (2) There is a solvation penalty (dielectric self-energy) for an ion as it enters the pore from the bath.<sup>19–21</sup> In our ion channel simulations, these two effects were taken into account indirectly by applying a smaller dielectric constant (typically 10) inside the protein surrounding the pore. The polarization surface charge density induced by ions and structural charges on the protein-pore boundary has effects that are qualitatively similar to the two effects of the small dielectric coefficient of the pore mentioned above. Although this boundary and the induced charge on it are present even if we decrease the dielectric coefficient inside the pore, these two effects could be studied directly. Simulations for multiple dielectrics along the permeation pathway in ion channels are in progress.

The electrochemical double layer (DL) consists of a charged surface (the electrode) and an electrolyte. It is usual to assume a layer with a low dielectric constant near the electrode to explain the experimental behavior of the DL capacitance. In our earlier paper, we simulated such a model at zero electrode charge, but we prevented the ions from penetrating into the low dielectric constant layer.<sup>9</sup> This was a reasonable assumption because ions are thought to be excluded from a

<sup>a)</sup> Author to whom correspondence should be addressed. Electronic mail: boda@almos.vein.hu.

compact water layer near the electrode. The assumption, however, is unreasonable for large electrode charges.

Torrie and Valleau<sup>4</sup> have performed simulations for DLs formed at the boundary layer of two immiscible electrolytes characterized by different dielectric coefficients. They assumed that the ions cannot leave their host electrolyte so the boundary between the two liquids acts as a hard wall for the ions. In reality, the interface between the two liquids is diffuse and ions can enter from one electrolyte to the other.

Apart from these examples, ions moving from one dielectric to another can probably occur in any inhomogeneous electrolyte system. The dielectric constant is reduced in an electrolyte where large electric fields act due to dielectric saturation. This can happen near charged electrodes, membranes, in confined systems, protein binding sites, at surfaces of charged colloid particles, or even in concentrated bulk electrolytes. It is known from the measurements of Barthel, Buchner and co-workers<sup>22,23</sup> that even the dielectric constant of homogeneous electrolytes decreases with increasing ion concentration so one would expect that inhomogeneous electrolyte systems with varying concentration are, at the same time, inhomogeneous with varying dielectric coefficient. These systems are difficult to calculate/simulate so even a reduced model with ions moving across the boundaries of piecewise dielectric domains is an important advance.

We mention a few exceptions from the literature, where ions passing through the boundary were not avoided. Graf and co-workers<sup>24,25</sup> used a Dynamic Lattice Monte Carlo (DLMC) simulation technique, where ions are only at lattice grid points. If the grid points are farther from the interface than the ion radius, the problem does not arise. Chung and co-workers<sup>26–28</sup> applied a one-particle potential in their Brownian Dynamics (BD) simulations to account for the dielectric penalty of an ion passing through an ion channel. In our earlier paper, we studied the problem of an ion passing through a single flat dielectric boundary using image charges.<sup>29</sup> This work provided only a partial solution to the problem as we will discuss later.

Image charges are useful mainly for the case of an infinite flat dielectric boundary and a few other simple symmetrical geometries.<sup>7,30,31</sup> For more general geometries, a numerical method is needed to compute the polarization surface charge induced on the dielectric boundaries. Various boundary element methods (BEM) in apparent surface charge (ASC) calculations were widely used to compute induced charges.<sup>32,33</sup> A variational formalism has been proposed by Allen *et al.*<sup>34</sup> Inspired by this paper, a method called the induced charge computation (ICC) method was proposed by us<sup>8,11</sup> and used to study DLs<sup>9</sup> and ion channels<sup>11,12,14,17</sup> with Monte Carlo (MC) simulations. In all these studies, the ions stayed in their native dielectric; they did not cross dielectric boundaries.

In this paper, we propose a method to treat ions crossing a dielectric boundary in the framework of the ICC method. For this, we need to step beyond the charged hard sphere model of the ion and use the concept of the “bubble ion” whose interior has a dielectric coefficient 1, so the surface of the ion is a polarizable surface. We will detail the different models of ions in Sec. II. We emphasize that while the “bubble ion” is conceptually a better model than the point charge (charged hard

sphere) model, it cannot be simulated because the calculation of the induced charge density on the ions’ surfaces is an unsurmountable task in a multi-particle simulation. This model is used as a tool to construct an interpolation mechanism to compute the energy as an ion is crossing through a dielectric boundary.

## II. MODEL OF ION

When we construct a molecular model for an ion immersed in an implicit solvent, we consider a charged object which is usually a sphere for simple inorganic ions. In the PM, the charge is a point charge in the center of the sphere. This sphere prevents ions from overlapping and, thus, prevents the point charges from approaching each other to an arbitrarily small distance. This feature of the model is not optional in computer simulations: ions must have finite size, otherwise the cations and anions would collapse into an infinitely small neutral particle and vanish from the simulation cell. In the PM, this is the only role of the sphere: the surface of the ion is electrostatically inactive; it does not appear in the solution of Poisson’s equation.

In reality, the surface of the ion separates two different dielectric media: the interior of the ion and the solvent around the ion. The ion has a subtle interaction with the dielectrics around it. For example, the electric field of the ion’s charge polarizes the solvent molecules around the ion. This manifests itself in a polarization charge density on the surface of the ion.

To model this, we consider a sphere of radius  $R$  immersed in a dielectric continuum of dielectric coefficient  $\epsilon$ . We assume that the system is infinite: the boundary condition of vanishing electric field at infinity is applied. Therefore, surface charges beyond those on the ion’s surface do not appear in the solution. The ion’s charge is the only source charge in the system and no external electric field is applied. We can represent the ionic charge in two ways:

1. We can place an ionic charge  $q$  on the surface of the ion as a uniform surface charge  $\sigma = q/4\pi R^2$  and not worry about the internal structure of the ion [Fig. 1(a)]. In this case, we solve Poisson’s equation for the domain outside the ion’s boundary surface:  $r \geq R$ , where the origin of the coordinate system is set at the center of the ion,  $r = |\mathbf{r}|$ . A net polarization charge  $q_{\text{pol}}$  is distributed on the surface of the ion as a uniform surface charge density with magnitude

$$\sigma_{\text{pol}} = \frac{q_{\text{pol}}}{4\pi R^2} = \left(\frac{1}{\epsilon} - 1\right) \frac{q}{4\pi R^2}. \quad (1)$$

This result can be obtained without any information about the internal structure of the ion.

2. We can place the charge in the center of the ion as a point charge  $q$  [Figs. 1(b)–1(e)]. In this case, we include the ion’s interior in the solution of Poisson’s equation. The surface of the ion then becomes a dielectric boundary. The distribution of the polarization charge  $q_{\text{pol}}$  depends on the dielectric coefficient inside the sphere,  $\epsilon_{\text{ion}}$  [Fig. 1(b)]. In this case, a polarization charge  $q_s$  is uniformly distributed on the surface of the ion with

magnitude

$$\sigma_s = \frac{q_s}{4\pi R^2} = \left( \frac{1}{\epsilon} - \frac{1}{\epsilon_{\text{ion}}} \right) \frac{q}{4\pi R^2}, \quad (2)$$

while a polarization charge appears on the central source charge as a point charge with magnitude

$$q_0 = \left( \frac{1}{\epsilon_{\text{ion}}} - 1 \right) q. \quad (3)$$

The sum of these two charges is equal to the total polarization charge:  $q_{\text{pol}} = q_0 + q_s$ .

If  $\epsilon_{\text{ion}} = 1$ , we talk about the “bubble ion” model, because there is a vacuum in the interior of the ion. In this case,  $\sigma_s = \sigma_{\text{pol}}$  and  $q_0 = 0$ , namely, all the polarization charge is on the surface of the ion [Fig. 1(c)].

If  $\epsilon_{\text{ion}} = \epsilon$ , the charged hard sphere model used in the PM is obtained [Fig. 1(d)]: the ion’s surface is not a dielectric boundary ( $\sigma_s = 0$ ) and all the polarization charge is concentrated in the center of the ion ( $q_0 = q_{\text{pol}}$ ). From outside, it looks like a point charge with an effective charge

$$q_{\text{eff}} = q + q_{\text{pol}} = \frac{q}{\epsilon}. \quad (4)$$

It is usual to assign values to  $\epsilon_{\text{ion}}$  that are larger than 1 thus taking the internal polarizability of the ion into account.<sup>31,35</sup> Even shells of different dielectric coefficients are in use to model ions and hydration shells around them.<sup>36,37</sup> We emphasize, however, that such ion models are not used in our simulations because they refer to polarizable ions. These models are mentioned merely to put the idea of the “bubble ion” into perspective.

Due to spherical symmetry, the solution of the electrostatic problem from Gauss’s law outside the sphere is the same in all cases. The integral form of Gauss’s law for any spherical surface  $A_r$  of radius  $r > R$  reads

$$\oint_{A_r} \mathbf{D} \cdot d\mathbf{a} = \oint_{A_r} \epsilon_0 \epsilon \mathbf{E} \cdot \mathbf{n} da = q, \quad (5)$$

from which the electric field is

$$\mathbf{E}(r) = \frac{q}{4\pi\epsilon_0\epsilon r^2} \mathbf{n}, \quad (6)$$

where  $\mathbf{n} = \mathbf{r}/r$  is the normal vector to surface  $A_r$  and  $\mathbf{D} = \epsilon_0\epsilon\mathbf{E}$  is the electric displacement. This solution is obtained no matter how we distribute the polarization charge between the ion’s center and its surface. What is more, the same result is obtained, if we distribute the charge as a volume charge inside the ion as soon as we do it in a spherically symmetric way.

The difference between the above models becomes clear when we place our “lonely” ion into an external electric field  $\mathbf{E}_{\text{ext}}(\mathbf{r})$  [Fig. 1(e)]. This external field is generally produced by other ions or any charged object (electrodes, for example). We can assume that  $\mathbf{E}_{\text{ext}}(\mathbf{r})$  has no source inside and on the surface of the ion. When this assumption is not valid, for example, in the case of an ion in contact with a charged surface or another “bubble ion,” the electrostatic problem must be solved by considering the two objects in contact together explicitly instead of including the effect of other charged objects in  $\mathbf{E}_{\text{ext}}(\mathbf{r})$ . Such contact positions are difficult electrostatic problems<sup>38</sup> to compute efficiently and precisely. Leaving these cases out of consideration, however, does not influence the derivation of our interpolation formulas.

The external electric field polarizes the dielectrics at the surface of the ion: a charge distribution  $\Delta\sigma(\mathbf{s})$  is induced on it, where  $\mathbf{s}$  is a vector on the ion’s surface [Fig. 1(e)]. The total polarization charge density on the ion’s surface is non-uniform

$$\sigma_{\text{tot}}(\mathbf{s}) = \sigma_s + \Delta\sigma(\mathbf{s}). \quad (7)$$

Because there is no source of  $\mathbf{E}_{\text{ext}}(\mathbf{r})$  in the domain  $r \leq R$  and the dielectric coefficient is uniform in that domain, the integral of  $\Delta\sigma(\mathbf{s})$  is zero (due to Gauss’s law), namely, the field only separates positive and negative charges. This zero-mean charge distribution corresponds to a multipole expansion whose dominant term is a dipole. On the molecular level, the charge distribution represents distortion of the structure of water molecules in the hydration shell with respect to their structure in the absence of  $\mathbf{E}_{\text{ext}}(\mathbf{r})$ . The non-uniform induced charge density  $\Delta\sigma(\mathbf{s})$  changes as the external electric field changes (because of, for example, the thermal movement of ions or any charged object).

The different models are polarizable to different degree: the point charge model ( $\epsilon_{\text{ion}} = \epsilon$ ) is not polarizable, while the “bubble ion” model ( $\epsilon_{\text{ion}} = 1$ ) is “fully” polarizable. In this case, the polarization charge density  $\sigma_{\text{pol}}$  on the surface of

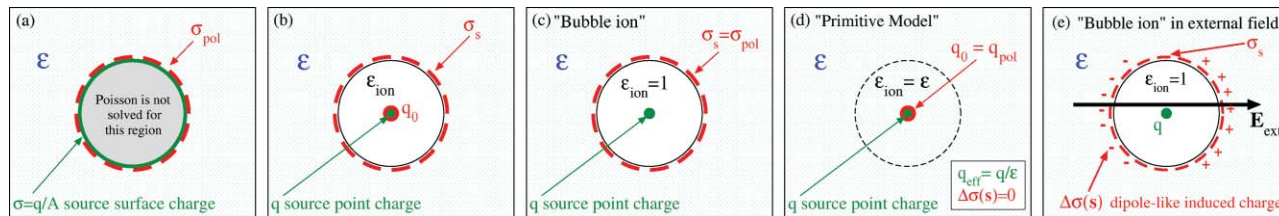


FIG. 1. Different models of an ion. In model (a), the ion carries a constant surface charge  $\sigma = q/A$ . Poisson’s equation is not solved for the interior of the ion. All the polarization charge is induced on the ion’s surface ( $\sigma_{\text{pol}}$ ). In models (b–d), the source charge is a point charge at the center of the ion. Polarization charges are induced either in the center of the ion ( $q_0$ ) or on the surface of the ion ( $\sigma_s$ ). When  $\epsilon_{\text{ion}} = 1$ , we talk about the “bubble ion” model (c). In this case, all the polarization charge is on the ion’s surface ( $\sigma_s = \sigma_{\text{pol}}$ ). When  $\epsilon_{\text{ion}} = \epsilon$ , all the polarization charge is in the center (d). This is the charged hard sphere model used in the PM: all the charge is in the center as an effective charge  $q_{\text{eff}} = q/\epsilon$ . When an external field is applied (e), all the ion models are polarizable (a dipole-like polarization charge  $\Delta\sigma$  appears on the surface), except the model (d) with  $\epsilon_{\text{ion}} = \epsilon$ . Because this latter model provides a pairwise additive pair potential, it can be used in simulations straightforwardly.



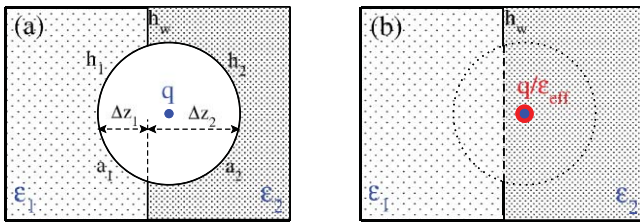


FIG. 2. The crossing ion (a) as a “bubble ion” and (b) the approximate way as an effective point charge with the overlapped portion of the boundary cut out. The area of the portion of the ion in dielectrics  $i$  is denoted by  $a_i$ . The polarization charge induced on it is denoted by  $h_i$ . The polarization charge induced on the dielectric wall outside the ion’s body is denoted by  $h_w$ .

the “bubble ion” represents the polarization of the surrounding medium, namely, the (mainly orientational) polarization of water molecules around the ion. The ion’s self polarizability does not appear in this model. The models in between ( $1 < \epsilon_{\text{ion}} < \epsilon$ ) are “partially” polarizable, where the ion’s self polarizability counteracts part of the water’s polarization.

The problem of the “bubble ion” [Fig. 1(e)] can be solved self-consistently by the ICC method. The problem of the crossing “bubble ion” [Fig. 2(a)] can also be solved by the ICC method. Solving the numerical problem in every step of the simulation is too expensive to be feasible, however. For that reason, the “bubble ion” model cannot be used in a computer simulation. It serves, however, as a useful concept to help in developing our interpolation technique to handle ions crossing the dielectric boundary in simulations.

The model that can be simulated is the one where the surface of the ion is not polarizable, namely, we assume that  $\Delta\sigma(\mathbf{s}) = 0$  [Fig. 1(d)]. The surface charge  $\sigma_s$  can then be squeezed into the center of the ion producing the effective charge in Eq. (4) representing the screening by the surrounding dielectric. This is the charge used in the screened Coulomb potential of the charged hard spheres of the PM. The surface of the ion is electrostatically inactive; only the hard wall remains that prevents ions from overlapping.

This model can be used straightforwardly when ions do not overlap with dielectric boundaries. The model, however, suffers from the problem of energy divergence as the ion crosses the dielectric boundary. In this paper, we present an interpolation technique inspired by the “bubble ion” model to overcome this difficulty. We discuss the errors produced by this approximation to an ion.

### III. THE INDUCED CHARGE COMPUTATION METHOD

The electrostatic problem can be treated by solving an integral equation using the induced charge density as an unknown variable instead of solving partial differential equations (the Poisson’s equation with boundary conditions) using the electrical potential as an unknown variable. The resulting ICC equation<sup>8,11</sup> is

$$\begin{aligned} \frac{\bar{\epsilon}(\mathbf{s})}{\Delta\epsilon(\mathbf{s})} h(\mathbf{s}) + \frac{1}{4\pi} \int_{\mathcal{B}} d\mathbf{s}' h(\mathbf{s}') \frac{(\mathbf{s} - \mathbf{s}') \cdot \mathbf{n}(\mathbf{s})}{|\mathbf{s} - \mathbf{s}'|^3} \\ = -\frac{1}{4\pi} \sum_k \frac{q_k}{\epsilon(\mathbf{r}_k)} \frac{(\mathbf{s} - \mathbf{r}_k) \cdot \mathbf{n}(\mathbf{s})}{|\mathbf{s} - \mathbf{r}_k|^3}, \end{aligned} \quad (8)$$

where  $\mathcal{B}$  is the entire dielectric boundary in the system (including the surfaces of the “bubble ions” if they are present),  $h(\mathbf{s})$  is the induced charge density,  $\bar{\epsilon}$  and  $\Delta\epsilon(\mathbf{s})$  are the mean and difference of the dielectric coefficients on the two sides of the boundary at  $\mathbf{s}$ , and  $\mathbf{n}(\mathbf{s})$  is the normal vector of the surface at point  $\mathbf{s}$ . The right-hand side of the equation is proportional to the normal electric field produced by the source point charges  $q_k$  in the system. The point charges are in positions  $\mathbf{r}_k$  in regions of dielectric coefficient  $\epsilon(\mathbf{r}_k)$ .

The solution of this equation is performed numerically by dividing the whole surface  $\mathcal{B}$  into surface elements  $\mathcal{B}_\alpha$  (tiles). Assuming that  $h_\alpha = h(\mathbf{s}_\alpha)$  is constant on the  $\alpha$ th tile, where  $\mathbf{s}_\alpha$  is the center of the  $\alpha$ th tile, the equation can be written for  $\mathbf{s}_\alpha$ ,

$$\begin{aligned} \sum_{\beta} h_{\beta} \left[ \frac{\bar{\epsilon}(\mathbf{s}_{\alpha})}{\Delta\epsilon(\mathbf{s}_{\alpha})} \delta_{\alpha\beta} + \frac{1}{4\pi} I_{\alpha\beta} \right] \\ = -\frac{1}{4\pi} \sum_k \frac{q_k}{\epsilon(\mathbf{r}_k)} \frac{(\mathbf{s}_{\alpha} - \mathbf{r}_k) \cdot \mathbf{n}(\mathbf{s}_{\alpha})}{|\mathbf{s}_{\alpha} - \mathbf{r}_k|^3}, \end{aligned} \quad (9)$$

where the integral

$$I_{\alpha\beta} = \int_{\mathcal{B}_{\beta}} d\mathbf{s}' \frac{(\mathbf{s}_{\alpha} - \mathbf{s}') \cdot \mathbf{n}(\mathbf{s}_{\alpha})}{|\mathbf{s}_{\alpha} - \mathbf{s}'|^3} \quad (10)$$

expresses the mutual polarization between tiles and takes into account the curvature of the tiles. This system of linear equations can be expressed as a matrix equation

$$\mathbb{A} \mathbf{h} = \mathbf{c}, \quad (11)$$

where matrix  $\mathbb{A}$  is defined by the expression in brackets in Eq. (9). The vector  $\mathbf{h}$  contains the surface charges at the tile centers, while vector  $\mathbf{c}$  contains the direct effect of the source charges (right-hand side of Eq. (9)). This latter quantity changes as ions move in the simulation; the induced charge can be obtained from a backsubstitution. The filling of the matrix and its LU decomposition [which writes the matrix as the product of a lower and an upper (LU) triangular matrix] is a very time consuming process. Therefore, this method is feasible only if the matrix  $\mathbb{A}$  can be precomputed and LU decomposed only once because it does not change in the simulation. This is the case when the dielectric boundary does not change its geometry in the simulation. If the moving ions carry dielectric boundaries on their surfaces (such as in the case of the “bubble ion”), this condition does not hold. The “bubble ion” model, therefore, is not practical in simulations.

Once the induced charge densities  $h_\alpha$  are computed, they are treated as point charges  $h_\alpha a_\alpha$  placed in the tile centers  $\mathbf{s}_\alpha$ , where  $a_\alpha$  is the area of the tile. The energy is then calculated from the usual Coulomb interactions. The discretized surface charge  $h_\alpha = h(\mathbf{s}_\alpha)$  is a representation of the total induced charge density on the ion’s surface  $\sigma_{\text{tot}}(\mathbf{s})$  introduced in Eq. (7).

The case of sharp dielectric boundaries is an idealization. In practice, dielectric boundaries are rather diffuse with the dielectric constant changing gradually over a finite region. This case, however, is computationally more expensive because a volume must be discretized into volume elements rather than just a surface into surface elements. For this reason, most authors use sharp dielectric boundaries in their models for simulations.

#### IV. INTERPOLATION OF ENERGY OF THE CROSSING ION

We will illustrate our idea by the example of a spherical ion crossing an infinite, flat boundary [Fig. 2(a)]. This system makes it possible to test the method in a simple geometry for which even an analytical solution is available. More extensive simulations for practical problems (ion channels, double layers) in comparison with experiments will be published later, but those comparisons would provide a check of the ion channel or the double layer model, not the simulation method (which is a goal here). We denote the position of the sphere's center with  $z$ , which is the coordinate perpendicular to the surface. The origin ( $z = 0$ ) is at the interface. The boundary separates two dielectric media with dielectric coefficients  $\epsilon_1$  and  $\epsilon_2$ . We denote the induced charge densities on the two portions of the ion's surface with which it is in dielectrics 1 and 2 by  $h_1$  and  $h_2$ , respectively. The areas of these spherical caps are  $a_1$  and  $a_2$ , respectively.

Before we describe the interpolation procedure, we establish two requirements that we expect from our methodology.

1. The first requirement is a consequence of the fact that we treat the ion as an effective point charge  $q_k/\epsilon(\mathbf{r}_k)$  at position  $\mathbf{r}_k$  with its surface not playing any part electrostatically [Fig. 1(d)] when it does not overlap the dielectric boundary. As boundary conditions for our interpolation mechanism, therefore, we expect from the method that it reproduces the point-charge solutions when the ion is in contact with the boundary on one or the other side ( $z = \pm R$  in Fig. 2(a)). We emphasize that the "bubble ion" model does not meet this requirement; it is only used as a useful concept to construct the mechanism.
2. The other requirement is additivity: if charge  $q_A$  (when alone) induces  $h_A$  polarization charge density on the dielectric boundaries and  $q_B$  (when alone) induces  $h_B$ , then the two charges (when they are present together) induce  $h_A + h_B$ .

Let us see, how a "bubble ion" behaves when it crosses a dielectric boundary [Fig. 2(a)]. First of all, when this happens, the electrostatic problem is solvable (with ICC, for example) and the energy of the ion changes continuously as the ion crosses the interface. If this is the only ion in the system, the energy changes continuously between two well-defined limiting values: the self energies of the ion in contact positions with the boundary in dielectrics 1 and 2. This self-energy has two parts: the interaction with the induced surface charges on the surface of the ion ( $h_1$  and  $h_2$ ) and with the induced surface charge on the dielectric boundary,  $h_w$ ,

$$U_s = U_s^{\text{ion}} + U_s^w. \quad (12)$$

Note that the boundary has a hole in it when an ion overlaps with it.

The first term of the self-energy,  $U_s^{\text{ion}}$ , has well-defined limiting values on the two sides of the surface, when the full body of the ion is in dielectric  $j$ ,

$$U_{s,j}^{\text{ion}} = \frac{q^2}{8\pi\epsilon_0 R} \left( \frac{1}{\epsilon_j} - 1 \right), \quad (13)$$

where  $\epsilon_j$  is the dielectric coefficient in region  $j$ . This is the well-known Born expression<sup>39</sup> for solvation of a spherical ion in a dielectric. In the "bubble ion" model, this equation is a direct consequence of Poisson's equation. This term is  $U_{s,1}^{\text{ion}}$  for  $z < -R$ , while it is  $U_{s,2}^{\text{ion}}$  for  $z > R$ . This interaction energy is negative and deeper in the dielectrics with larger  $\epsilon_j$ .

The self-energy  $U_{s,j}^{\text{ion}}$  of a point charge used in the PM diverges ( $\lim_{R \rightarrow 0} U_{s,j}^{\text{ion}} = -\infty$ ), because the ion's induced charge is infinitely close to the central point charge. This does not cause any problem in calculations using the PM in one phase, because this term does not change as ions move in their host dielectric  $\epsilon_j$ . When the ion changes its dielectric environment, i.e., goes from one phase to another; however, this term must be taken into account. We assume that the ion has a finite self-energy (solvation energy, see Ref. 40)  $U_{s,j}^{\text{ion}}$  despite the fact that we treat the ion as a point charge in the simulation. Therefore, we can meet requirement 1, if we establish the limiting values  $U_s^{\text{ion}}(z = -R) = U_{s,1}^{\text{ion}}$  and  $U_s^{\text{ion}}(z = R) = U_{s,2}^{\text{ion}}$  as given by Eq. (13).

Between these limiting values,  $U_s^{\text{ion}}(z)$  changes continuously as the ion crosses the boundary, because the common areas of the ionic surface with dielectrics 1 and 2 ( $a_1$  and  $a_2$ ) change continuously [see Fig. 2(a)],

$$U_s^{\text{ion}}(z) = \frac{1}{8\pi\epsilon_0} \frac{q}{R} q_{\text{tot}}(z), \quad (14)$$

where

$$q_{\text{tot}}(z) = \int_{a_1} h_1 da + \int_{a_2} h_2 da \quad (15)$$

is the total induced charge on the surface of the ion. In general,  $q_{\text{tot}}(z)$  depends on  $z$  through all the variables  $h_1(z)$ ,  $h_2(z)$ ,  $a_1(z)$ , and  $a_2(z)$ . We assume, however, that the induced charge densities on the areas  $a_1$  and  $a_2$  depend, to first order, only on  $q$ ,  $R$ , and  $\epsilon_j$  in the following way [see Eq. (1)]:

$$h_j = \frac{q}{4\pi R^2} \left( \frac{1}{\epsilon_j} - 1 \right), \quad (16)$$

so they can be taken to be constant and independent of  $z$ . This assumption means that we take into account the polarizing effect of only the central charge; the cross polarization effects between the charges on the whole dielectric boundary  $\mathcal{B}$  (expressed by the non-diagonal elements of matrix  $\mathbb{A}$ ) are ignored. Because the non-diagonal elements of the matrix  $\mathbb{A}$  are small compared to the diagonal elements, this assumption is reasonable and results in a solely geometrical problem,

$$q_{\text{tot}}(z) = h_1 a_1(z) + h_2 a_2(z), \quad (17)$$

namely, we only need to determine the areas  $a_i(z)$ . (The approximation of the surface induced charge neglecting the off-diagonal entries of the ICC matrix has been studied in detail elsewhere and called the BIBEE model.<sup>41</sup>) For a flat boundary [Fig. 2(a)], the solution is straightforward, because the area  $a_j = 2\pi R \Delta z_j$  of a spherical cap of height  $\Delta z_j$  is proportional to  $z$ . The resulting equations for  $a_i(z)$  are

$$\begin{aligned} a_1(z) &= 2\pi R(R - z), \\ a_2(z) &= 2\pi R(R + z). \end{aligned} \quad (18)$$

These equations imply that  $q_{\text{tot}}(z)$  and  $U_s^{\text{ion}}(z)$  also change linearly in the region of overlap.

As far as the other term of the self-energy, the interaction with the induced charge density on the wall,  $h_w$ , is concerned, the limiting values  $U_s^w(z = \pm R)$  are also well defined. These values are the interactions of the effective point charge  $q_j/\epsilon_j$  placed at  $z = \pm R$  with the polarization charge density induced by itself on the dielectric boundary (calculated, for example, with ICC). Between these limiting values, the term  $U_s^w(z)$  changes continuously, because the geometry of the dielectric boundaries changes continuously as the “bubble ion” is crossing the boundary. Note that divergence does not occur because the  $\epsilon_{\text{ion}} = 1$  interior of the “bubble ion” always separates the central charge from the boundary.

In general, the dielectric boundary is not necessarily a single, flat boundary. It can be (1) curved and (2) it is possible that more than two boundaries meet along a line (the ion channel geometry, studied in subsequent papers, is an example). We can generalize Eq. (17) for such cases as

$$q_{\text{tot}}(\mathbf{r}) = \sum_i h_i a_i(\mathbf{r}). \quad (19)$$

Based on the approximation in Eq. (19), we suggest the following interpolation scheme to compute the energy of the system when an ion overlaps with the boundary.

(1) In the first step, we shrink the induced charge  $q_{\text{tot}}$  into the ion’s center as a point charge [Fig. 2(b)]. In this case, the surface of the ion becomes electrostatically inactive shown by the dotted sphere in Fig. 2(b). Merging this induced charge  $q_{\text{tot}}(\mathbf{r})$  with the source charge  $q$ , we define the effective charge in the center of the ion and, through this, we define an effective dielectric coefficient  $\epsilon_{\text{eff}}(\mathbf{r})$ ,

$$q_{\text{eff}}(\mathbf{r}) = q + q_{\text{tot}}(\mathbf{r}) = \frac{q}{\epsilon_{\text{eff}}(\mathbf{r})}. \quad (20)$$

From Eqs. (16), (19) and (20) we obtain that

$$\frac{1}{\epsilon_{\text{eff}}(\mathbf{r})} = \sum_i \frac{a_i^*(\mathbf{r})}{\epsilon_i}, \quad (21)$$

where  $a_i^*(\mathbf{r}) = a_i(\mathbf{r})/4\pi R^2$  is the fraction of area  $a_i(\mathbf{r})$  from the whole ion-surface in  $\epsilon_i$  (a normalized surface). This corresponds to computing the ionic self-energy in the usual way using the effective dielectric coefficient

$$U_s^{\text{ion}}(\mathbf{r}) = \frac{q^2}{8\pi\epsilon_0 R} \left( \frac{1}{\epsilon_{\text{eff}}(\mathbf{r})} - 1 \right). \quad (22)$$

We perform this interpolation for every point  $\mathbf{r}$  of the simulation cell. This way, the effective dielectric coefficient can be obtained as a position-dependent quantity  $\epsilon_{\text{eff}}(\mathbf{r})$ . This interpolation has to be performed for every ion species, because the radii of each species is different. If a more complex dielectric boundary is present (if the boundaries are curved, for example),  $\epsilon_{\text{eff}}(x_l, y_m, z_n)$  can be precomputed on a grid at the beginning of the simulation, tabulated, and interpolated for an arbitrary  $\mathbf{r}$  during the simulation.

(2) In the next step, we show how to compute this problem with the ICC method. Most importantly, the subsurface of the dielectric boundary inside the ion’s body, namely, where the ion overlaps with the dielectric boundary (shown by

dashed line in Fig. 2(b)), has to be removed when we compute the induced charge density of the overlapping ion. This is easy conceptually, but more difficult in practice. Because the matrix  $\mathbb{A}$  takes so long to build and invert, we would rather not change it by removing the overlapping tiles. Below we outline an approximate way to accomplish the same thing without changing the matrix.

The overlapping tiles must be left in the calculation when we compute the induced charge density of a non-overlapping ion. This a consequence of requirement 2: the induced charge densities of the overlapping and non-overlapping ions must be additive. So, if the overlapping ion is not present, the induced charge density of the non-overlapping ion must be computed with the dielectric boundary intact. This means that the induced charge density of the non-overlapping ion must be computed for every surface element whether or not another ion might overlap with that surface element time to time.

Due to additivity, the ICC equation [Eq. (8)] can be solved using individual ions as source charges separately (the sum over  $k$  on the right-hand side is absent). The right-hand side of such an equation is computed as

$$c_{\alpha,k} = \begin{cases} 0, & \text{if } |\mathbf{s}_\alpha - \mathbf{r}_k| \leq R_k, \\ -\frac{1}{4\pi\epsilon_{\text{eff}}(\mathbf{r}_k)} \frac{q_k (\mathbf{s}_\alpha - \mathbf{r}_k) \cdot \mathbf{n}(\mathbf{s}_\alpha)}{|\mathbf{s}_\alpha - \mathbf{r}_k|^3}, & \text{if } |\mathbf{s}_\alpha - \mathbf{r}_k| > R_k, \end{cases} \quad (23)$$

where  $R_k$  is the radius of the  $k$ th ion. With this approach we eliminate the direct polarizing effect of an ion on the tiles that are overlapped with this particular ion (the distance of ion center and tile center is smaller than the ion radius). The polarization effects of other tiles on these overlapping tiles is still nonzero (because we use the original matrix  $\mathbb{A}$ ) but they are small. In this way, we do not have to recompute the matrix; the method does not impose any additional cost on the computation apart from computing  $\epsilon_{\text{eff}}(\mathbf{r})$ . Computing  $\epsilon_{\text{eff}}(\mathbf{r})$ , however, is fast compared to computing the induced charge  $\mathbf{h}$ . Note that  $\epsilon_{\text{eff}}(\mathbf{r}_k)$  is used in Eq. (23) as the dielectric coefficient of the ion at position  $\mathbf{r}_k$ .

Then, the polarization charge density,  $h_{\alpha,k}$  induced by ion  $k$  on surface element  $\alpha$  can be obtained from a LU backsubstitution. The total induced charge density on tile  $\alpha$  can be obtained as a sum over the ions

$$h_\alpha = \sum_k h_{\alpha,k}, \quad (24)$$

where the sum is taken for ions that do not overlap with the surface element  $\alpha$ .

The interaction energy between two ions is

$$u_{ij}^{\text{ion-ion}}(\mathbf{r}_i, \mathbf{r}_j) = \frac{q_i q_j}{8\pi\epsilon_0 |\mathbf{r}_i - \mathbf{r}_j|} \left( \frac{1}{\epsilon_{\text{eff}}(\mathbf{r}_i)} + \frac{1}{\epsilon_{\text{eff}}(\mathbf{r}_j)} \right). \quad (25)$$

The interaction energy between an ion and an induced charge in the center of a tile is

$$u_{i\alpha}^{\text{ion-ind}}(\mathbf{s}_\alpha, \mathbf{r}_i) = \begin{cases} 0, & \text{if } |\mathbf{s}_\alpha - \mathbf{r}_i| \leq R_i, \\ \frac{q_i h_\alpha a_\alpha}{8\pi\epsilon_0 |\mathbf{s}_\alpha - \mathbf{r}_i|}, & \text{if } |\mathbf{s}_\alpha - \mathbf{r}_i| > R_i. \end{cases} \quad (26)$$



With this equation, we eliminate the interaction of an ion with the tiles that overlap with it mimicking the bubble ion. The total energy is

$$U = \sum_i \sum_{j<i} u_{ij}^{\text{ion-ion}} + \sum_i \sum_{\alpha} u_{i\alpha}^{\text{ion-ind}}. \quad (27)$$

## V. RESULTS FOR AN ION CROSSING A FLAT DIELECTRIC BOUNDARY

Our procedure is illustrated by the example of a spherical ion (with radius  $R$ ) crossing an infinite, flat, and sharp dielectric boundary separating two regions with dielectric coefficients  $\epsilon_1$  and  $\epsilon_2$  (Fig. 3). There is another ion in a fixed position  $z_f = -4R$  with an effective point charge  $q_f/\epsilon_1$  and a crossing ion whose center is at coordinate  $z$ . We will plot our results as functions of this variable. The charge of the crossing ion is  $q_c$  in the “bubble ion” model in the center of the bubble together with the induced charge densities on the bubble’s surface ( $h_1, h_2$ ), while it is a  $q_c/\epsilon_{\text{eff}}(z)$  effective charge in the interpolation method. In this study, we use the elementary charge for both the crossing and the fixed ion:  $q_c = q_f = e$ . Using other values does not influence our main conclusions.

We will study the induced charge densities (and the interaction energies with them) on three distinct dielectric boundaries: (1) the ion’s surface in dielectric  $\epsilon_1$ , (2) the ion’s surface in dielectric  $\epsilon_2$ , and (3) the flat dielectric boundary outside the ion’s body. We denote the induced charge densities (induced by  $q$ ) on these surfaces by  $h_{1,q}$ ,  $h_{2,q}$ , and  $h_{w,q}$ , respectively. We report charges in the unit of the elementary charge, while we report the energies in unit of  $e^2/R$ .

We use the ICC method<sup>8</sup> to compute the induced charges. For this, the surface of the dielectric boundary must be discretized into surface elements ( $B_\alpha$ ). We performed this discretization with the method given in the supplementary material of Ref. 11. On the surface of the ion and on the flat dielectric boundary near the ion we defined surface elements of the size roughly  $0.16 \times 0.16$  (in  $R$  unit). Using finer grid does not influence our results very much. For the numerical method, we must represent the otherwise infinite surface with a finite sheet. We used a circular sheet of radius  $30R$ . The finite size of the discretized dielectric boundary is the main source of inaccuracies compared to analytical values (that, in some cases, can be obtained from the image charge method). This small inaccuracy, however, if we keep its reason in mind, does not influence our main conclusions.

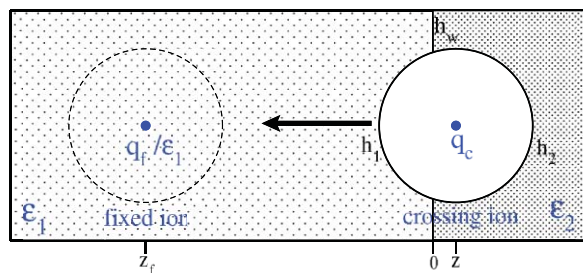


FIG. 3. An ion of charge  $q_c$  is crossing the dielectric boundary (separating regions  $\epsilon_1 = 20$  and  $\epsilon_2 = 80$ ) and approaching an ion with effective charge  $q_f/\epsilon_1$  at fixed position  $z_f = -4R$ .

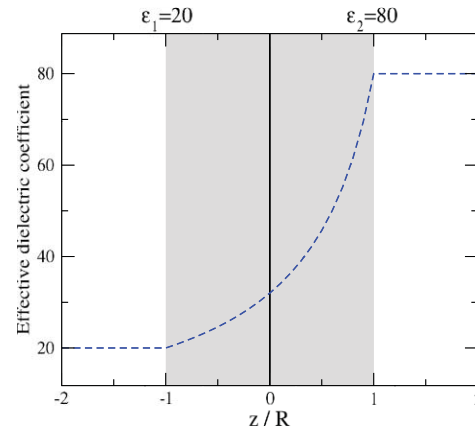


FIG. 4. The effective dielectric coefficient profile as computed from Eq. (28) for  $\epsilon_1 = 20$  and  $\epsilon_2 = 80$ .

While “bubble ions” are computationally prohibitive in simulations, it is feasible to calculate the energies of two such ions near each other with one crossing the dielectric boundary in a model case. We do this using the ICC method where the matrix  $\mathbb{A}$  is recalculated and inverted for every position of the moving ion. Symbols in subsequent figures represent these calculations. Solid lines, on the other hand, represent results of the interpolation scheme, when the crossing ion is a point charge  $q/\epsilon_{\text{eff}}(\mathbf{r})$ . Outside the overlapping region (represented by area of gray shade in the figures), this is the way as we normally compute energy in simulations for the PM. Therefore, solid lines at contact positions,  $z = \pm R$ , represent the limiting values for the energies between which the interpolation must work.

The profile of the effective dielectric coefficient as computed from Eqs. (18) and (21) is

$$\epsilon_{\text{eff}}(z) = \begin{cases} \epsilon_1, & \text{if } z \leq -R, \\ \frac{1}{2} \left( \frac{1-z/R}{\epsilon_1} + \frac{1+z/R}{\epsilon_2} \right)^{-1}, & \text{if } -R < z < R, \\ \epsilon_2, & \text{if } z \geq R, \end{cases} \quad (28)$$

and plotted in Fig. 4.

The polarization charges induced by the crossing ion integrated over three distinct dielectric boundaries are plotted in Fig. 5. The total induced charge on the ion’s surface is  $1/\epsilon_1 - 1 = -0.95$  on the left-hand side ( $z \leq -R$ ), while it is  $1/\epsilon_2 - 1 = -0.9875$  on the right-hand side ( $z \geq R$ ). These are the limiting values for the total induced charges  $\int_{a_1(z)} h_{1,q_c} da$  and  $\int_{a_2(z)} h_{2,q_c} da$ . These functions change linearly with  $z$  between the limiting values in the case of the interpolation method (see Eqs. (17) and (18)) as shown by the red and green solid lines. In particular,  $\int_{a_1(z)} h_{1,q_c} da$  changes linearly between  $1/\epsilon_1 - 1$  (when  $a_1 = 4\pi R^2$ ) and 0 (when  $a_1 = 0$ ). The exact solutions for the “bubble ion” are plotted by symbols (open red circles and green squares) and agree with the interpolated results very well. This indicates that the approximation introduced in Eq. (19) is reasonable.

The total induced charge on the flat dielectric boundary (which has a hole, when the ion overlaps with it) also has two well-defined limiting values:  $(\epsilon_1 - \epsilon_2)/\epsilon_1(\epsilon_1 + \epsilon_2) = -0.03$

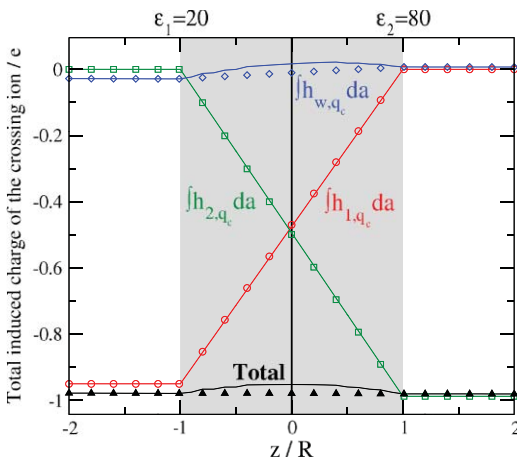


FIG. 5. The total polarization charge induced by the crossing ion,  $q_c = e$ , on the left ( $\int_{a_1} h_{1,q_c} da$ ) and right ( $\int_{a_2} h_{2,q_c} da$ ) spherical caps of the crossing ion and on the dielectric boundary outside the body of the ion ( $\int h_{w,q_c} da$ ) as functions of the  $z$ -coordinate (in  $R$ -unit) of the crossing ion. In this figure and following figures, symbols represent results for the “bubble ion” model, while solid lines represent results obtained with the interpolation scheme for  $|r| < R$  and with the point charge model for  $|r| \geq R$ .

for  $z \leq -R$  and  $(\epsilon_2 - \epsilon_1)/\epsilon_2(\epsilon_1 + \epsilon_2) = 0.0075$  for  $z \geq R$ . The total charge in the overlap region ( $|z| < R$ ) changes almost linearly in the “bubble ion” model (open blue diamonds), while the shape of the interpolated curve (solid blue line) is different from this linear solution (the same is valid for the total charge – black curve and triangles). The main source of the deviation is the assumption that the  $q_c/\epsilon_{\text{eff}}(z)$  effective charge has the same polarizing effect on the dielectric boundary as the “bubble ion” has. The result, however, obeys the boundary conditions at  $z = -R$  and  $z = R$  and produces a continuous curve between the limiting values.

We denote the interaction energy of  $q_i$  with the polarization charge induced by  $q_j$  on a given segment of the dielectric boundary by  $U(q_i - h_{\gamma,q_j})$ , where  $i$  and  $j$  denotes the crossing or the fixed ion (c or f) and  $\gamma$  denotes the segment (1, 2, or w). Figure 6 shows the interaction energies of  $q_c$  with its own induced charges induced on the various segments of the dielectric boundary. The energies  $U(q_c - h_{1,q_c})$  and  $U(q_c - h_{2,q_c})$  behave the same way as the total induced charges  $\int_{a_1} h_{1,q_c} da$  and  $\int_{a_2} h_{2,q_c} da$  (compare the top panel of Fig. 6 with Fig. 5) because the distance of  $q_c$  from  $h_{1,q_c}$  (and also from  $h_{2,q_c}$ ) is constant ( $R$ ). The figure shows the solution that we obtain by assuming that the ions are point charges (dashed lines). For this special case, these curves can be (and are) calculated with the image charge method.

The next term,  $U(q_c - h_{w,q_c})$ , is the one that causes the divergence problem when point charges are used. Outside the overlapping region, the three models (“bubble ion,” interpolation, and point charge) give practically (apart from numerical errors) identical results. In the overlapping region, the point-charge curves diverge as  $|z| \rightarrow 0$ , while the interpolation gives a curve that is quite similar to the “bubble ion” result and changes smoothly between the limiting values. The same is true for the sum of these energies.

The polarization charge induced by the other, fixed ion is shown in Fig. 7. The induced charges on the spherical caps,  $\int_{a_1} h_{1,q_f} da$  and  $\int_{a_2} h_{2,q_f} da$ , indicate a zero-mean dipole-like

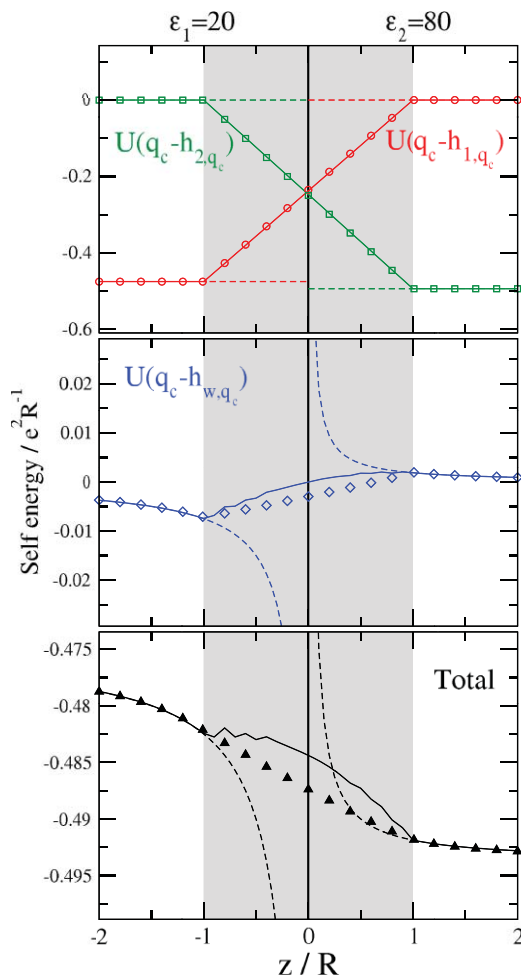


FIG. 6. The interaction energy of charge  $q_c$  with the polarization charge induced by itself (self-energy) as a function of the position of the crossing ion ( $z$ ). Interactions with the charge on the left ( $\int_{a_1} h_{1,q_c} da$ ) and right ( $\int_{a_2} h_{2,q_c} da$ ) spherical caps are shown in the top panel. Interaction with the charge induced on the dielectric boundary outside the body of the ion ( $\int h_{w,q_c} da$ ) is shown in the middle panel. The total interaction energy is shown in the bottom panel. The meaning of symbols and solid lines is the same as in Fig. 5. Here and in subsequent figures, the dashed lines represent results of image charge calculations assuming that the crossing ion is a point charge.

distribution in the “bubble-ion” model (magnified in the inset). The total induced charge on the left and right caps are positive and negative, respectively, and they are equal in magnitude as they are supposed to be according to Gauss’s law. These charges separately are not distinguished in the interpolation method, while their sum is taken to be zero (solid black line).

The total polarization charge on the flat boundary,  $\int h_{w,q_c} da$ , is constant in the interpolation method according to our assumption of additivity. It is independent of the position of the crossing ion. The “bubble ion” model reproduces this result within 0.4% error. The deviation (hidden by the scale of the figure) is due to the finite size of the flat boundary used in the ICC calculations.

The interaction energy of the crossing charge ( $q_c$ ) with the polarization charges induced by the fixed ion ( $q_f/\epsilon_1$ ) is shown in Fig. 8. The interactions with the charges on the spherical caps (top panel) reflect the behavior of the total induced charges (Fig. 7) on these caps because the distance of  $q_c$



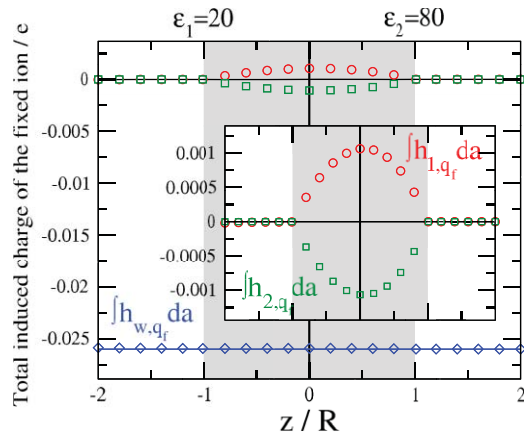


FIG. 7. The total polarization charge induced by the fixed ion,  $q_f = e$ , on the left ( $\int_{a_1} h_{1,q_f} da$ ) and right ( $\int_{a_2} h_{2,q_f} da$ ) spherical caps of the crossing ion and on the dielectric boundary outside the body of the ion ( $\int h_{w,q_f} da$ ) as functions of the  $z$ -coordinate of the crossing ion. The meaning of symbols and lines is the same as in Fig. 6.

from these charges is constant ( $R$ ). The interaction with  $h_{w,q_f}$  shows interesting behavior (bottom panel). The interpolation method yields a symmetrical curve because the interaction depends on  $|z|$ . The jumps in the curve are due to the nature of discretization of the flat dielectric boundary. As the crossing ion proceeds through the boundary, the surface element with which it overlaps vanishes from the calculation abruptly because this overlap is checked by the distance from the center of the surface element.

The “bubble ion” model provides a smooth curve, but it is not symmetrical for the following reason. The “bubble ion” is polarized by  $q_f$ : a dipole-like charge distribution appears on its surface. This induced dipole is larger when the crossing ion is closer to the fixed ion. This dipole has an additional polarizing effect on the flat dielectric boundary: it changes  $h_{w,q_f}$ . In the “bubble ion” model, the requirement for additivity, therefore, is not fulfilled. It makes sense to talk about additivity only if the dielectric boundaries do not change as ions move. In the “bubble ion” model, however, the dielectric boundary is changed as the “bubble ion” moves in space. Furthermore, the “bubble ion” model does not meet the other requirement either: it does not reproduce the limiting values at  $z = -R$  and  $z = R$  (also because of the induced dipole). These limiting values are the values given by the solid curves at  $z = \pm R$  in all the figures. These facts show that the “bubble ion” model is here being used only as a helpful concept to develop the interpolation mechanism. It could be used (in theory) to compute the energy in the overlap-region, but only if we use the same model outside the overlap-region too. Because this is too time consuming, we use the point charge model on the two sides of the overlap-region and an interpolation scheme in between.

The image charge solution neglects the size of the crossing ion (dashed line). Outside the overlap-region, the solution agrees with the numerical solution (apart from numerical errors). As the point charge approaches the dielectric boundary, its interaction with the surface charge induced by another ion approaches a finite value. This interaction term, therefore, is not a source of the divergence despite the fact that the point charge gets infinitely close to the charge on the wall. The im-

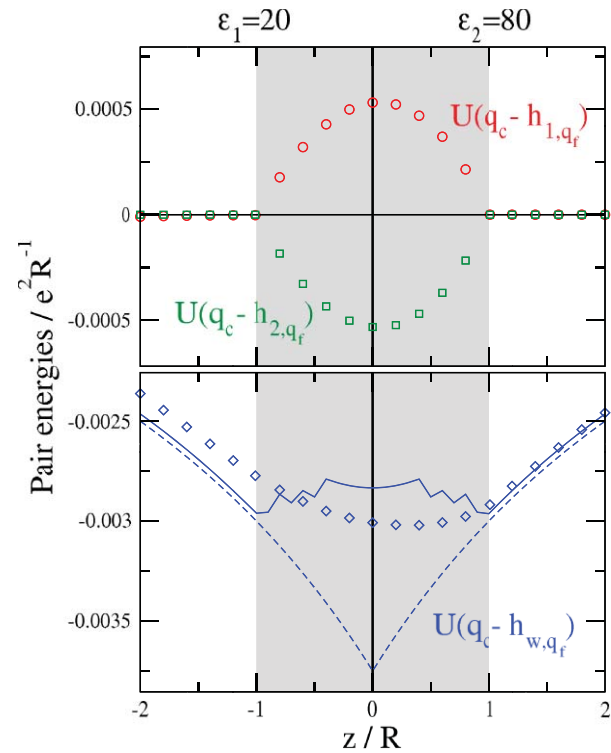


FIG. 8. The interaction energy of the crossing charge  $q_c$  with the polarization charge induced by the fixed ion  $q_f$  as a function of the position of the crossing ion ( $z$ ). Interactions with the charge on the left,  $U(q_c - h_{1,q_f})$ , and right,  $U(q_c - h_{2,q_f})$ , spherical caps are shown in the top panel. Interaction with the charge induced on the dielectric boundary outside the body of the ion,  $U(q_c - h_{w,q_f})$ , is shown in the bottom panel. The meaning of symbols and lines is the same as in Fig. 6.

age charge solution, therefore, could be a suitable approximation for this energy term. As a matter of fact, we used this approximation in our earlier study<sup>29</sup> though, at that time, we were not aware of all the subtleties discussed in this work.

The interaction energy of the fixed charge ( $q_f$ ) with the polarization charge of the crossing charge ( $h_{\gamma,q_c}$ ) also shows an interesting behavior (Fig. 9). The top panel shows the interaction of  $q_f$  with the charges on the spherical caps. The curves show a behavior similar to those for the  $U(q_c - h_{1,q_c})$  and  $U(q_c - h_{2,q_c})$  interactions (see top panel of Fig. 6) except that the limiting values differ more on the two sides now because not only are the charges different in the two positions, but also the distance of  $q_f$  from the spherical caps (this distance was  $R$  in the case of the  $U(q_c - h_{1,q_c})$  and  $U(q_c - h_{2,q_c})$  interactions).

The sum of these two energy terms gives a smooth curve in the case of the “bubble ion” and the interpolated models. The agreement between them is excellent. The point charge solution, however, shows a jump in the interaction energy at the interface (dashed line, see inset of the top panel). This solution was obtained by computing the interaction with the induced charge on the crossing point-charge ion; this induced charge is also a point charge of magnitude  $(1/\epsilon_i - 1)q_c$  “on top” of the ionic point charge  $q_c$ . The jump in  $\epsilon_i$  explains the jump in the interaction energy between  $q_f$  and this charge.

The interaction energy with  $h_{w,q_c}$  also changes continuously in the “bubble ion” and the interpolation models

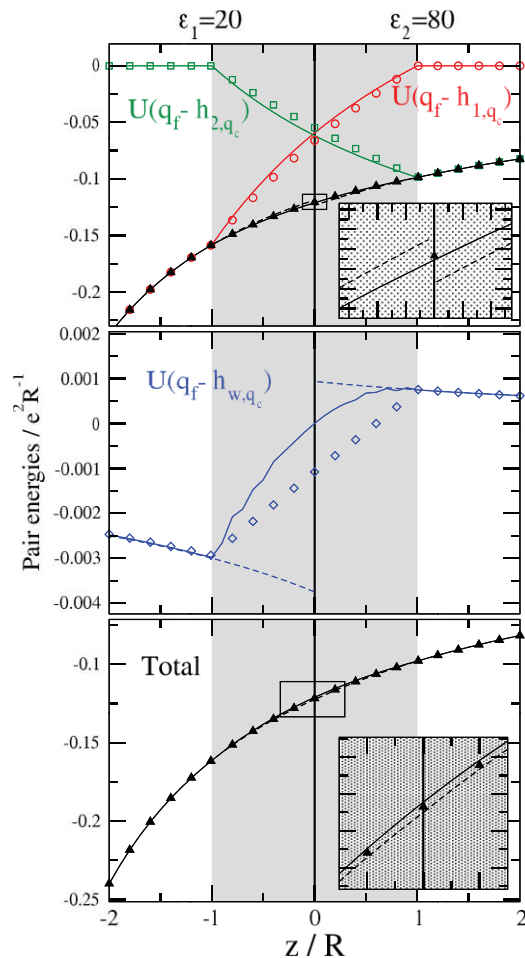


FIG. 9. The interaction energy of the fixed charge  $q_f$  with the polarization charge induced by the crossing ion  $q_c$  as a function of the position of the crossing ion ( $z$ ). Interactions with the charge on the left,  $U(q_f - h_{1,q_c})$ , and right,  $U(q_f - h_{2,q_c})$ , spherical caps are shown in the top panel. Interaction with the charge induced on the dielectric boundary outside the body of the ion,  $U(q_f - h_{w,q_c})$ , is shown in the middle panel. The total interaction energy is shown in the bottom panel. Insets magnify the region close to the boundary. The meaning of symbols and lines is the same as in Fig. 6.

(middle panel). Again, the point charge solution (computed from image charges) has a jump at the interface. This is because the  $h_{w,q_c}$  surface charge is induced by a  $q_c/\epsilon_1$  effective charge on the left-hand side, while it is induced by a  $q_c/\epsilon_2$  effective charge on the right-hand side. The abrupt jump in  $\epsilon_i$  results in a jump in  $h_{w,q_c}$  and, consequently, in the interaction energy  $U(q_f - h_{w,q_c})$ .

The sum of these terms, however, results in a smooth function (bottom panel), not only in the numerical solutions (“bubble ion” and interpolation models), but also in the point charge solution. The two jumps in the top and middle panels compensate each other. This also justifies our simplified treatment in our earlier work.<sup>29</sup> In a general case, however, a simple solution from image charges is not available. In such cases, a numerical method and the algorithm that interpolates for the overlap-region is necessary.

The interaction energy of the fixed ion ( $q_f$ ) with its own induced charge ( $h_{\gamma,q_f}$ ) is shown in Fig. 10. For the “bubble ion” model, the interaction with the charge on the ion’s surface (black triangles in the top panel) increases as the cross-

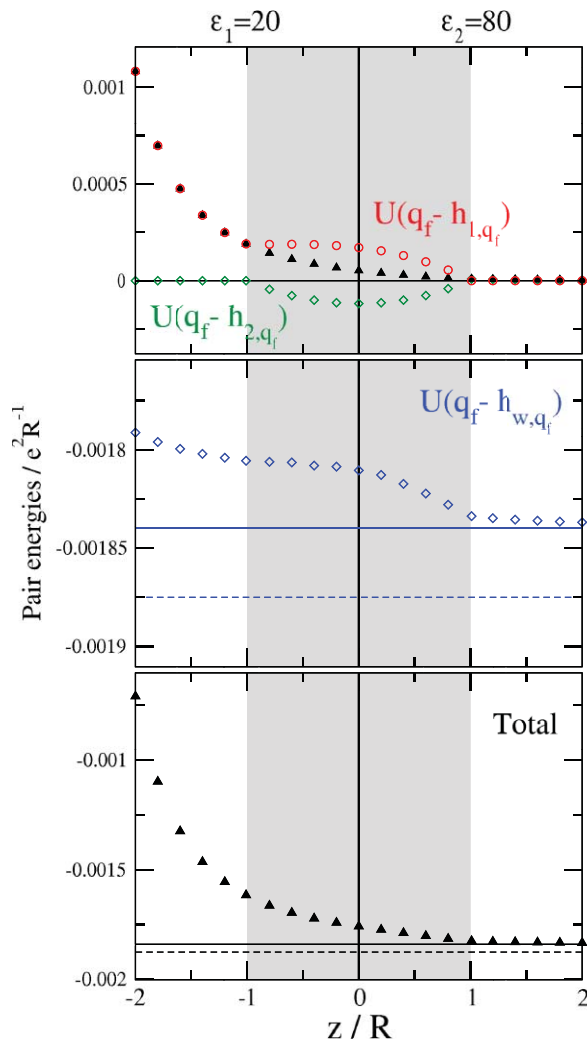


FIG. 10. The interaction energy of the fixed charge  $q_f$  with the polarization charge induced by itself as a function of the position of the crossing ion ( $z$ ). Interactions with the charge on the left,  $U(q_f - h_{1,q_f})$ , and right,  $U(q_f - h_{2,q_f})$ , spherical caps are shown in the top panel. Interaction with the charge induced on the dielectric boundary outside the body of the ion,  $U(q_f - h_{w,q_f})$ , is shown in the middle panel. The total interaction energy is shown in the bottom panel. The meaning of symbols and lines is the same as in Fig. 6.

ing ion approaches the fixed ion. The explanation, again, is that the fixed ion polarizes the crossing ion. This energy term reflects the interaction of  $q_f$  with the induced dipole on the crossing ion. In the interpolation model, this energy is zero, because the ion is not polarizable, so the induced dipole does not appear.

The interaction with the induced charge on the dielectric wall is obviously constant in the interpolation method (solid line in the middle panel). It is different from the image charge solution (dashed line) due to the finite size of the boundary used in ICC. The “bubble ion” model shows a deviation from this constant (symbols) because of the polarizing effect of the induced dipole on the wall (same effect as in the bottom panel of Fig. 8).

The total interaction energy between  $q_f$  and its induced charge (bottom panel) shows a considerable increase as the crossing “bubble ion” approaches the fixed ion due mainly to

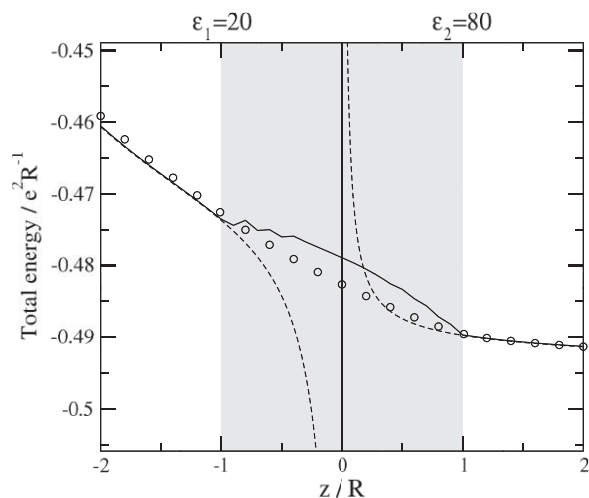


FIG. 11. Total energy of the system as a function of the position of the crossing ion ( $z$ ). This energy contains the direct interaction between the two charges ( $q_c q_f / |z_f - z_c|$ ) and the interaction between  $q_c$  and the induced charge on  $q_f$  ( $0.5q_c(1/\epsilon_1 - 1)q_f / |z_f - z_c|$ ) in all methods.

the interaction with the induced dipole. Because the model ions we study are not polarizable, this solution is not appropriate for our purpose.

The total energy is the sum of all the electrostatic energies in the system (Fig. 11): the sum of the charge – induced charge energies plotted in Figs. 6, 8–10 plus the direct interaction energy between the two charges. The interaction energy between  $q_c$  and the induced charge on  $q_f$  must also be added: it is a point charge and the interaction can be expressed analytically (see the caption of Fig. 11). The figure is quite similar to the bottom panel of Fig. 6, so as a general conclusion we can state that the main source of the inaccuracy of the interpolation method is the self-energy.

## VI. CONCLUSIONS

We have proposed a general scheme for simulation of ions crossing a sharp dielectric boundary in the implicit solvent framework. The ions are modeled as point charges embedded inside the body of the ion. The dielectric coefficient is the same inside and outside the ions, while the induced charge appears on top of the point source charge also as a point charge. This model can be simulated straightforwardly because the computation of the source charge – induced charge interactions does not require resources in addition to the source charge – source charge interactions. In this study, we considered spherical ions with the charges in the centers of the spheres defined by hard sphere potential (PM of electrolytes). It is straightforward, however, to extend the model for non-spherical ions.

We have reported detailed results for an ion crossing a flat boundary, but the procedure is given (and has been programmed) for dielectric boundaries of any shape. As a matter of fact, we applied the method for our ion channel geometry where there is a penetrable dielectric boundary between the solution inside and outside the channel. Using the point charge approach without the interpolation method described

here, the ions that approach the dielectric boundary from the low dielectric side are trapped in low-energy positions (the diverging self-energy is attractive in this case, see Fig. 6 left from the interface). These trapped ions result in high unphysical peaks in the simulation. Using the interpolation method, however, we obtained density profiles that behave smoothly in the neighborhood of the dielectric boundary. We will report these results in subsequent papers along with checks on the procedure with curved boundaries. Numerical checks need to be done on actual curved surfaces, because procedures can fail on curve boundaries that work well on flat ones, as we have discussed previously.<sup>11</sup>

We have reported the results using the ICC method to treat dielectric boundaries and induced charge densities. The general scheme, however, can be used for any other Poisson equation solver.

## ACKNOWLEDGMENTS

The authors acknowledge the support of the Hungarian National Research Fund (OTKA K75132). The work was supported in part by National Institutes of Health (NIH) Grant No. GM076013. The authors are grateful for the helpful comments of Jay Bardhan.

- <sup>1</sup>T. Croxton, M. D. A., G. N. Patey, G. M. Torrie, and J. P. Valleau, *Can. J. Chem.* **59**, 1998 (1981).
- <sup>2</sup>G. M. Torrie, J. P. Valleau, and G. N. Patey, *J. Chem. Phys.* **76**, 4615 (1982).
- <sup>3</sup>G. M. Torrie, J. P. Valleau, and C. W. Outhwaite, *J. Chem. Phys.* **81**, 6296 (1984).
- <sup>4</sup>G. M. Torrie and J. P. Valleau, *J. Electroanal. Chem.* **206**, 69 (1986).
- <sup>5</sup>D. Bratko, B. Jönsson, and H. Wennerström, *Chem. Phys. Lett.* **128**, 449 (1986).
- <sup>6</sup>P. Linse, *J. Phys. Chem.* **90**, 6821 (1986).
- <sup>7</sup>R. Messina, *J. Chem. Phys.* **117**, 11062 (2002).
- <sup>8</sup>D. Boda, D. Gillespie, W. Nonner, D. Henderson, and B. Eisenberg, *Phys. Rev. E* **69**, 046702 (2004).
- <sup>9</sup>D. Henderson, D. Gillespie, T. Nagy, and D. Boda, *Mol. Phys.* **103**, 2851 (2005).
- <sup>10</sup>S. Grandison, R. Penfold, and J.-M. Vanden-Broeck, *Phys. Chem. Chem. Phys.* **7**, 3486 (2005).
- <sup>11</sup>D. Boda, M. Valiskó, B. Eisenberg, W. Nonner, D. Henderson, and D. Gillespie, *J. Chem. Phys.* **125**, 034901 (2006).
- <sup>12</sup>D. Boda, M. Valiskó, B. Eisenberg, W. Nonner, D. Henderson, and D. Gillespie, *Phys. Rev. Lett.* **98**, 168102 (2007).
- <sup>13</sup>M. M. Hatlo and L. Lue, *Soft Matter* **4**, 1582 (2008).
- <sup>14</sup>D. Boda, M. Valiskó, D. Henderson, B. Eisenberg, D. Gillespie, and W. Nonner, *J. Gen. Physiol.* **133**, 497 (2009).
- <sup>15</sup>J. Reščič and P. Linse, *J. Chem. Phys.* **129**, 114505 (2008).
- <sup>16</sup>Z. Y. Wang and Y. Q. Ma, *J. Chem. Phys.* **131**, 244715 (2009).
- <sup>17</sup>D. Boda, J. Giri, D. Henderson, B. Eisenberg, and D. Gillespie, *J. Chem. Phys.* **134**, 055102 (2011).
- <sup>18</sup>R. D. Coalson and M. G. Kurnikova, *IEEE Trans. Nanobiosci.* **4**, 81 (2005).
- <sup>19</sup>M. H. Cheng and R. D. Coalson, *J. Phys. Chem. B* **109**, 488 (2005).
- <sup>20</sup>B. Corry, S. Kuyucak, and S.-H. Chung, *Biophys. J.* **84**, 3594 (2003).
- <sup>21</sup>T. Baştuğ and S. Kuyucak, *Biophys. J.* **84**, 2871 (2003).
- <sup>22</sup>J. Barthel, R. Buchner, and M. Münsterer, *DECHEMA Chemistry Data Series* (DECHEMA, Frankfurt a.M., 1995), Vol. 12.
- <sup>23</sup>R. Buchner, G. T. Hefter, and P. M. May, *J. Phys. Chem. A* **103**, 1 (1999).
- <sup>24</sup>P. Graf, A. Nitzan, M. G. Kurnikova, and R. D. Coalson, *J. Phys. Chem. B* **104**, 12324 (2000).
- <sup>25</sup>P. Graf, M. G. Kurnikova, R. D. Coalson, and A. Nitzan, *J. Phys. Chem. B* **108**, 2006 (2004).
- <sup>26</sup>S.-H. Chung, T. W. Allen, M. Hoyles, and S. Kuyucak, *Biophys. J.* **77**, 2517 (2001).



- <sup>27</sup>B. Corry, T. W. Allen, S. Kuyucak, and S.-H. Chung, *Biophys. J.* **80**, 195 (2001).
- <sup>28</sup>T. Vora, B. Corry, and S.-H. Chung, *Biochim. Biophys. Acta* **1668**, 106 (2005).
- <sup>29</sup>D. Boda, T. Varga, D. Henderson, D. D. Busath, W. Nonner, D. Gillespie, and B. Eisenberg, *Mol. Simul.* **30**, 89 (2004).
- <sup>30</sup>R. Kjellander and S. Marčelja, *J. Chem. Phys.* **82**, 2122 (1985).
- <sup>31</sup>S. Gavryushov, *J. Phys. Chem. B* **111**, 5264 (2007).
- <sup>32</sup>H. Hoshi, M. Sakurai, Y. Inoue, and R. Chûjô, *J. Chem. Phys.* **87**, 1107 (1987).
- <sup>33</sup>J. P. Bardhan, R. S. Eisenberg, and D. Gillespie, *Phys. Rev. E* **80**, 011906 (2009).
- <sup>34</sup>R. Allen, J. P. Hansen, and S. Melchionna, *Phys. Chem. Chem. Phys.* **3**, 4177 (2001).
- <sup>35</sup>S. Gavryushov and P. Linse, *J. Phys. Chem. B* **107**, 7135 (2003).
- <sup>36</sup>M. H. Abraham and J. Liszi, *J. Chem. Soc., Faraday Trans. I* **74**, 1604 (1978).
- <sup>37</sup>M. H. Abraham and J. Liszi, *J. Chem. Soc., Faraday Trans. I* **76**, 1219 (1980).
- <sup>38</sup>J.-Q. Feng, *Phys. Rev. E* **62**, 2891 (2000).
- <sup>39</sup>M. Born, *Z. Phys.* **1**, 45 (1920).
- <sup>40</sup>J. Vincze, M. Valiskó, and D. Boda, *J. Chem. Phys.* **133**, 154507 (2010).
- <sup>41</sup>J. P. Bardhan, *J. Chem. Phys.* **129**, 144105 (2008).